Effects of the atmospheric dynamic and thermodynamic fields on the eastward propagation of Tibetan Plateau vortices

By LUN LI[1]*, RENHE ZHANG[2,3], MIN WEN[1], JIANPING DUAN[4], and YANJUN QI[1], [1]*State Key Laboratory of Severe Weather, Chinese Academy of Meteorological Sciences, Beijing, China;* [2]*Institute of Atmospheric Sciences, Fudan University, Shanghai, China;* [3]*CAS Center for Excellence in Tibetan Plateau Earth Sciences, Beijing, China;* [4]*Institute of Atmospheric Physics, Chinese Academy Science, Beijing, China*

ABSTRACT

Tibetan Plateau vortices (TPVs) are major rain-producing systems over the Tibetan Plateau. Some TPVs can move off the plateau under certain conditions and impact rainfall over Eastern China. Accordingly, the eastward propagation distances of the TPVs moving off the plateau (EPDs) are closely related to the areas of rainfall associated with TPVs. In this study, the moving-off TPVs during May-August of 1998–2015 are classified into two groups according to their EPDs, and the circulations and heating fields at the times when the TPVs move off the plateau (i.e. moving-off times) are investigated based on reanalysis data. The dynamic and thermodynamic conditions to the east of the Tibetan Plateau are found to significantly impact the EPDs. In the middle and lower troposphere, the zonal ranges of negative geopotential height anomalies to the east of the Tibetan Plateau are in accordance with the EPDs of the TPVs, indicating that anomalous lows play a favourable role in the eastward movement of TPVs. In addition, the anomalous highs to the northeast of the Tibetan Plateau and over Southeastern China also benefit the maintenance of cyclonic circulation to the east of the plateau. Meanwhile, in the upper troposphere, the jet stream over Northeast Asia is beneficial for divergence at 200 hPa. Accordingly, ascending motion associated with the upper-level divergence and lower-level convergence is observed, with the zonal extent corresponding well to the EPDs in the two situations. The atmospheric thermodynamic factors also show a remarkable effect on the EPDs. The TPVs move farther away when the unstable stratification and water vapour convergence extend further eastward. The heating ranges above 500 hPa coincide with the EPDs of TPVs, implying a close relationship between the heating fields and the EPDs. These results benefit prediction on EPDs and further on rainfall to the east of the Tibetan Plateau.

Keywords: Tibetan Plateau vortices, eastward propagation distance, dynamic and thermodynamic fields, large-scale circulation, heating field

1. Introduction

Tibetan Plateau vortices (TPVs) are major mesoscale rain-triggering systems that form over the Tibetan Plateau at 500 hPa (Ye and Gao, 1979). Most TPVs originate over the central-western plateau between June and August, and far fewer initialize in May and September; the occurrence frequency of TPVs reaches its maximum in June (Luo, 1992). The typical spatial scale of TPVs is ∼400–800 km in the horizontal direction and 2–3 km in the vertical direction (Ye and Gao, 1979; Lhasa Workgroup for Tibetan Plateau Meteorology Research, 1981; Luo, 1992; Luo et al., 1994). The cyclonic circulation associated with TPVs is primarily in the middle-lower troposphere, with positive vorticity reaching a maximum at 500 hPa and disappearing above 400 hPa (Ye and Gao, 1979; Lhasa Workgroup for Tibetan Plateau Meteorology Research, 1981). Most TPVs dissipate in situ in 12–24 h; however, some can persist for longer durations and move eastward out of the plateau (Wang et al., 2009). The TPVs moving off the plateau are often

closely related to the generation of southwest vortices in Southwestern China (Li et al., 2017), and these TPVs trigger heavy rainfall to the east of the Tibetan Plateau and can cause disastrous weather events over Eastern China (Ye and Gao, 1979; Qiao and Zhang, 1994; Li, 2002).

Previous studies on moving-off TPVs have focused mainly on their eastward propagation over the Tibetan Plateau and the large-scale circulations benefiting the eastward movement of TPVs have been revealed. At 200 hPa, the divergence associated with the eastward moving upper-level westerly jet stream and the eastward stretching South Asia high is an important factor in the eastward movement of TPVs (Liu and Fu, 1985; Yu et al., 2007). At 500 hPa, the eastward movement of TPVs is accompanied by a northward-shifting monsoon trough over the Bay of Bengal, a westward-extending western Pacific subtropical high (WPSH) and active shear lines over the eastern Tibetan Plateau (Guo, 1986; Gao and Yu, 2007; Gu et al., 2010). Liu and Fu (1985) noted that three types of TPVs could move off the plateau, including TPVs existing behind a ridge, in front of a westerly trough, and on a shear line. Convergence to the east of the TPVs at 500 hPa between the northwesterly winds invading the northern region of the Tibetan Plateau and southwesterly winds originating from the Bay of Bengal is a prominent factor modulating the eastward movement of TPVs (Li et al., 2011; Li et al., 2014a). Water vapour is another important factor affecting the eastward movement of TPVs. TPVs move eastward when the water vapour convergence centre in the middle-upper troposphere is located over the eastern side of the TPVs (Yu, 2002). Regarding the thermodynamic fields, some studies have stated that the latent heat of condensation is the leading factor in the development of TPVs (Dell'Osso and Chen, 1986; Wang, 1987; Li et al., 2011; Li et al., 2014b), while some highlighted the role of surface sensible heating (Lhasa Workgroup for Tibetan Plateau Meteorology Research, 1981; Shen et al., 1986; Li and Zhao, 2002; Luo et al., 1991) and considered that the dynamic effect is less important (Luo and Yang, 1992; Chen et al., 1996). In addition, the moving-off TPVs are significantly dominated by the 10–20-day quasi-biweekly oscillation (QBWO), and TPVs always move off the Tibetan Plateau in positive QBWO phases (Li et al., 2018).

Moving-off TPVs influence precipitation over broad areas of China. The active period of sustained moving-off TPVs occurs from June to August, and these TPVs are always generated near Qumalai (96°E, 34°N) (Yu et al., 2014). After moving off the Tibetan Plateau, the directions of TPVs are modulated mainly by the positive vorticity variability to the east of the TPVs (Xiao et al., 2016).

The number of eastward moving TPVs is positively related to rainfall over the middle-upper reaches of the Yangtze River, the upper reaches of the Yellow River and the region of the Yangtze-Huaihe Rivers (Huang et al., 2015). In addition, the moving-off TPVs between the WPSH and the high to the southeast of Lake Baikal exert the most remarkable effect on rainfall in China (Yu et al., 2015).

Previous studies have investigated the mechanisms of the development and eastward movement of TPVs over the Tibetan Plateau and the characteristics of TPVs after they move off the Tibetan Plateau. As introduced above, the activities of TPVs moving off the Tibetan Plateau have a close relationship with the rainfall over the regions to the east of the plateau, including even the Korean Peninsula and Japan (Yu and Gao, 2006). Considering that the eastward propagation distances of the TPVs and the rainfall to the east of the Tibetan Plateau are closely related, in this study, the moving-off TPVs are classified into two groups according to their eastward propagation distances beyond the Tibetan Plateau (EPDs), and the effects of the atmospheric dynamic and thermodynamic fields on the EPDs are investigated. The aim of this work is to reveal the features of the large-scale circulations and heating fields that determine how far the TPVs move beyond the Tibetan Plateau. The results are beneficial for predicting the EPDs and which regions may be influenced by the precipitation related to TPVs. The data and methods utilized in this work are introduced in Section 2. The features of the atmospheric dynamic fields are shown in Section 3. In Section 4, we compare the thermodynamic fields corresponding to the two groups of TPVs. A summary and discussion are given in Section 5.

2. Data and methods

2.1. Data

The ERA-interim data used in the present study to investigate the large-scale circulations and thermodynamic factors are derived from the European Centre for Medium-Range Weather Forecasts (ECMWF), with global coverage and an approximate $0.7° \times 0.7°$ horizontal resolution at a 6-h interval for May–August in 1998–2015 (Dee et al., 2011). The 12-h accumulated precipitation data observed at 00 UTC and 12 UTC by 2474 stations in the same period are used here, which are obtained from the daily surface dataset provided by the China Meteorological Data Service Center (CMDC). Details on these data can be found at http://idata.cma/idata/web/data/index?dataCode = SURF_CHN_MUL_DAY, through which the dataset can also be downloaded. In this study, the anomalies of the variables are calculated by subtracting
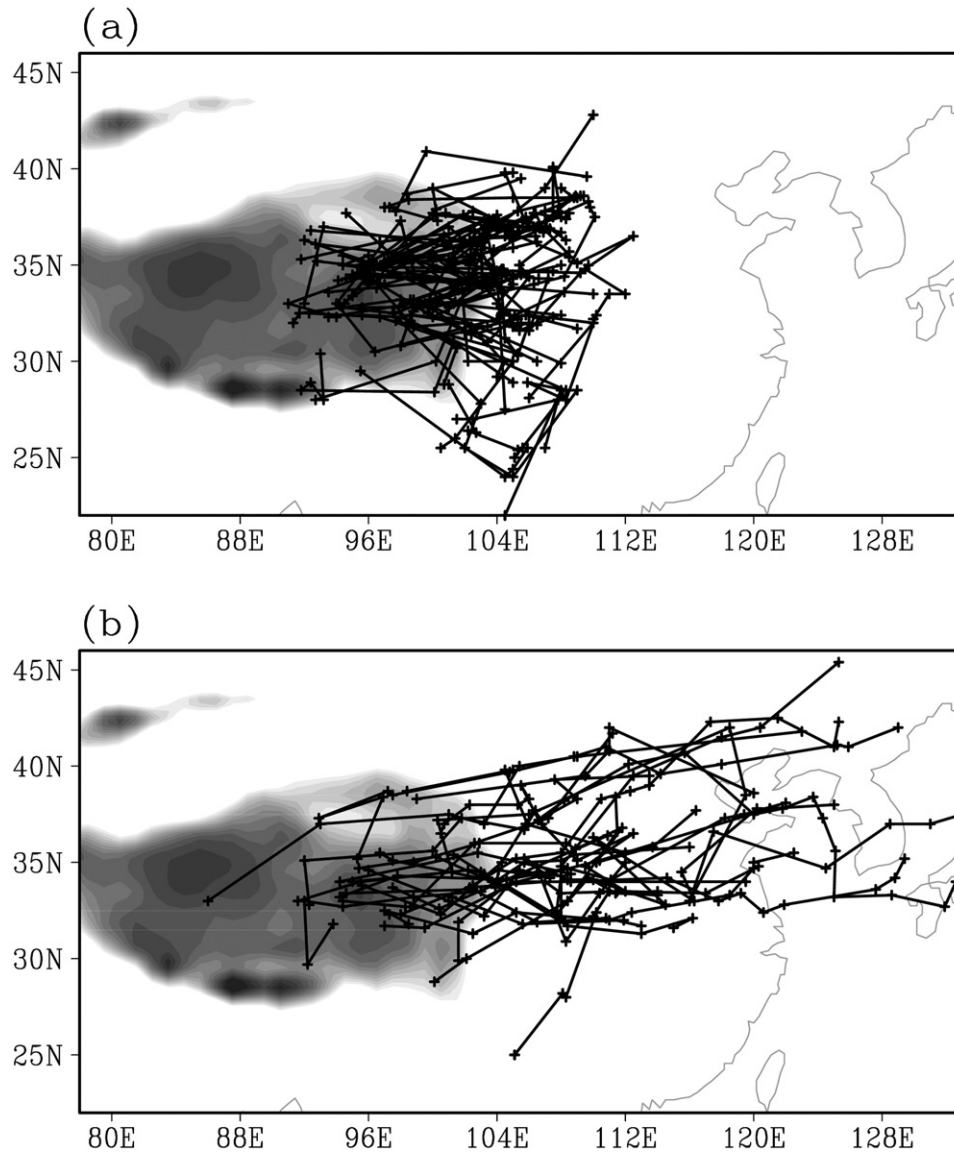
Fig. 1. Tracks of the two groups of moving-off TPVs classified according to the EPDs. The upper (a) and lower (b) panels correspond to situation W and situation E, respectively. Shading indicates areas with altitude over 3000 m. The cross (+) in each track denotes the centre position of the vortex at a time interval of 12 h.

their climatological means from the original data. To highlight the features of the large-scale circulations and the heating fields, considering that the lifetimes of the moving-off TPVs are primarily less than 3 days, 3-day running means of the dynamic and thermodynamic factors discussed in this work are calculated to smooth the signals of TPVs.

2.2. Definition of TPVs and TPVs composites

According to previous research (Lhasa Workgroup for Tibetan Plateau Meteorology Research, 1981), the definition of TPVs is based on the 500 hPa geopotential height or wind fields. Accordingly, a low forming over the Tibetan Plateau with closed contours in the 500 hPa geopotential height field, or with cyclonic winds at 500 hPa at three observation stations is defined as a TPV. The moving-off TPVs are selected by referring to the *Yearbook of Tibetan Plateau Vortex and Shear Line* from the Institute of Plateau Meteorology, China Meteorological Administration (CMA), which covers the period 1998 to 2015. The yearbooks exhibit the activities of all of the TPVs forming over the Tibetan Plateau, providing observational information of the TPVs (Yu et al.,
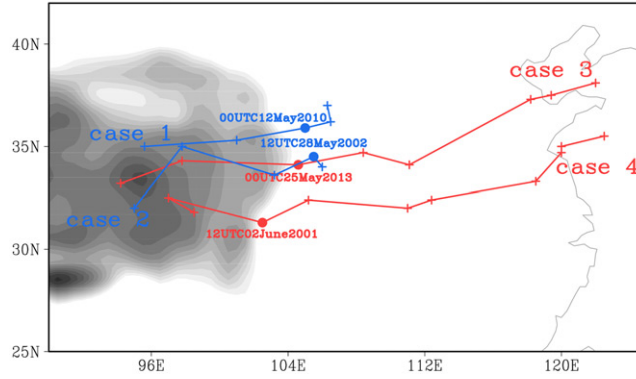
Fig. 2. Two TPVs with short EPDs (case 1 and case 2) and two TPVs with long EPDs (case 3 and case 4). The cross (+) in each track denotes the centre position of the vortex at a time interval of 12 h. The locations of TPVs at the moving-off times are dotted. Shading indicates areas with altitude over 3000 m.

2012; Tang et al., 2014; Li et al., 2018). In the present study, a moving-off TPV is defined as a TPV moving eastward and shift out of the plateau region, where the elevation exceeds 3000 m. The selected moving-off TPVs are classified into two groups according to their EPDs (Fig. 1). The TPVs that dissipate to the west of 110°E are defined as group W, and those reaching beyond 110°E are defined as group E. The two zonal ranges above correspond to the upper, middle and lower reaches of the Yangtze River, respectively. The situations corresponding to these two groups of TPVs are marked as "situation W" and "situation E" for short.

It should be emphasized that the EPDs in this study refer to the distances of the TPVs from the Tibetan Plateau after moving off. The main focus is on the pre-existing conditions to the east of the Tibetan Plateau. Thus, the dynamic and thermodynamic fields at the moving-off times are composed. Here, the moving-off time is defined as the first time after a TPV moves off the Tibetan Plateau. Therefore, the moving-off time is the time just after the TPVs move off but before further eastward propagation.

To show the moving-off time and the composite method clearly, four cases are given for example. Figure 2 includes two cases with short EPDs (case 1 and case 2) and two cases with long EPDs (case 3 and case 4). The moving-off times of these four cases are presented in Fig. 2, and the locations of the TPVs at the moving-off times are dotted. The moving-off times of cases 1 and 2 are 00UTC12May2010 and 12UTC28May2002, respectively, and those of cases 3 and 4 are 00UTC25May2013 and 12UTC02June2001. The dynamic fields (e.g., winds and geopotential height at 500 and 700 hPa, wind speed at 200 hPa, and vertical motion) and thermodynamic fields (e.g. potential pseudo-equivalent temperature, water vapour condition

and atmospheric apparent heat source) on 00UTC12May2010 and 12UTC28May2002 (00UTC25May2013 and 12UTC02June2001) are composed, and the results are considered as the conditions corresponding to the TPVs with short (long) EPDs. The dynamic and thermodynamic fields at the moving-off times of all of the cases in group W and group E are composed, respectively, in the same way stated above.

Accordingly, the large-scale circulations and thermodynamic fields in Figs. 4–12 are all related to the composites at the moving-off times of the TPVs.

2.3. Water vapour flux

The water vapour condition is closely related to the latent heat of condensation; thus, the vertically integrated water vapour flux is calculated using the following equation (Rasmusson, 1968):

$$A = \frac{1}{g} \int_{P_u}^{P_s} q\boldsymbol{V} \mathrm{d}p \tag{1}$$

A and $\boldsymbol{V}$ denote the water vapour flux and the horizontal wind vector, respectively. P_s is the pressure at the ground, and P_u is the pressure of the upper level; in this study, P_u=300 hPa. q represents the specific humidity.

2.4. Atmospheric apparent heat source and apparent moisture sink

The atmospheric apparent heat source (Q_1) and the apparent moisture sink (Q_2) are calculated based on the atmospheric thermodynamic equation and the moisture equation, respectively. The equations used are as follows (Yanai et al., 1973):

$$Q_1 = c_p \left(\frac{\partial T}{\partial t} + \boldsymbol{V} \bullet \nabla T + \omega \left(\frac{P}{P_0} \right)^{\kappa} \frac{\partial \theta}{\partial p} \right) \tag{2}$$
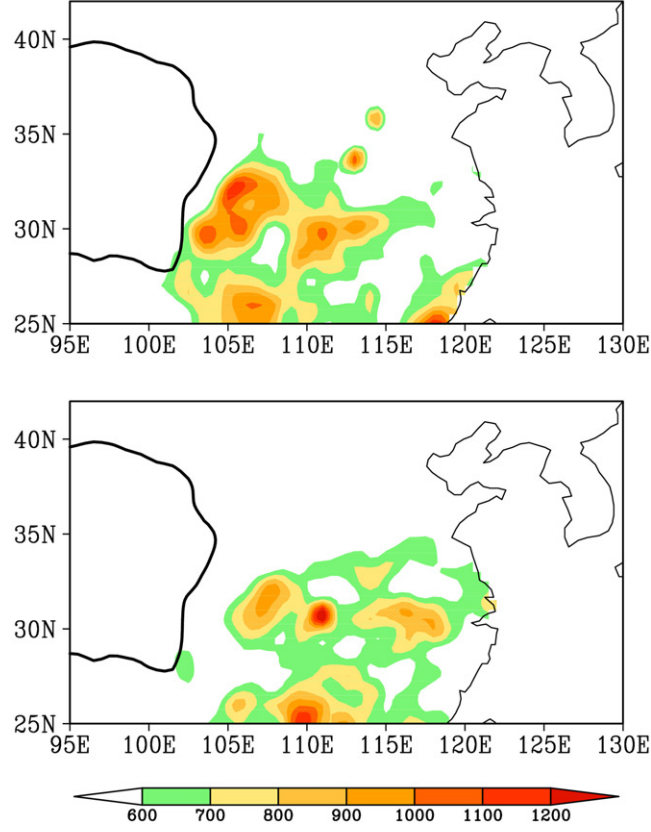
Fig. 3. Accumulated rainfall after the TPVs move off the plateau in (a) situation W and (b) situation E (unit: cm). The black line represents the topographic contour of 3000 m.

$$Q_2 = -L\left(\frac{\partial q}{\partial t} + \boldsymbol{V} \bullet \boldsymbol{\nabla} q + \omega \frac{\partial q}{\partial p}\right) \qquad (3)$$

where T is the temperature and $\boldsymbol{V}$ and ω denote the horizontal wind vector and the vertical wind component in pressure coordinates, respectively. P_0 is the pressure of 1000 hPa. c_p represents the specific heat at a constant pressure, and $\kappa \approx 0.286$. θ is the potential temperature. $L = 2.5\text{x}10^6$ J kg^{-1}, denoting the latent heat of condensation. The vertically integrated forms of Equations (2) and (3) can be written as follows:

$$< Q_1 > \approx LP + S + < Q_R > \qquad (4)$$

$$<Q_2> \approx LP - LE \qquad (5)$$

where P, S, and E represent the amount of precipitation, surface sensible heat flux, and eddy moisture flux, respectively, and $<Q_R>$ denotes radiative heating (cooling). Generally, similar values and distributions of Q_1 and Q_2 imply that LP (the latent heat of condensation) is the major component of Q_1.

3. Atmospheric dynamic features

The accumulated rainfall after the TPVs move off the Tibetan Plateau is shown in Fig. 3. The centres of rainfall are found southeast of the tracks of the two groups of TPVs. In both situations, one rainfall centre is observed near the Tibetan Plateau, corresponding to the stage when the TPVs are not far from the Tibetan Plateau, while another is observed over the middle and lower reaches of the Yangtze River. In situation W, the TPVs dissipate to the west of 110°E (Fig. 1a); accordingly, the rainfall centres associated with the moving-off TPVs are mainly located over Southwestern China (Fig. 3a). In situation E (Fig. 3b), the zonal range of the precipitation is from 105°E to 120°E, which stretches further eastward than it does in situation W. Clearly, the TPVs with longer EPDs influence precipitation over broader regions. Thus, precipitation to the east of the Tibetan Plateau is closely related to the EPDs of the TPVs.

3.1. Middle and lower troposphere

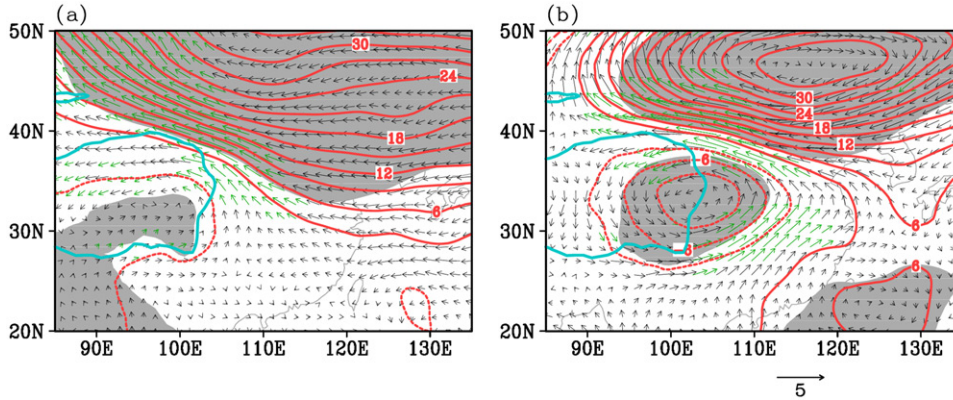Composites of 500 hPa winds and geopotential height anomalies are presented in Fig. 4. Negative geopotential

Fig. 4.   Composites of the 500 hPa anomalous winds (vectors; unit: m s^{-1}) and geopotential height (contours; unit: gpm) in (a) situation W and (b) situation E. The cyan line represents the topographic contour of 3000 m. The geopotential height anomalies with statistical significance exceeding the 90% confidence level are shaded, and winds exceeding the 90% confidence level are coloured with green.

height anomalies are found to the east of the Tibetan Plateau in both situations (the negative value in situation W is minimal, thus it is not displayed in Fig. 4a). In general, in the Northern Hemisphere, low-pressure systems correspond to convergence field. Previous study (Li et al., 2019) revealed that the convergence at 500 hPa to the east of TPVs contributes to positive potential vorticity tendency, which favours the maintenance of moving-off TPVs. Moreover, both the intensity and extent of the negative geopotential height anomalies are considerably larger in situation E (Fig. 4b) than in situation W (Fig. 4a), corresponding to longer EPDs in the former relative to the latter (Fig. 1). In both situations, an anomalous high exists to the northeast of the Tibetan Plateau, which is centred further south in situation E. The related southeasterly winds anomalies to the southwest of the anomalous high are beneficial for the existence of an anomalous cyclonic circulation to the east of the Tibetan Plateau. In particular, positive geopotential height anomalies are observed over Southeastern China in situation E, indicating a stronger WPSH compared with that in situation W. The southwesterly anomalies associated with the WPSH, in conjunction with the southeasterly winds anomalies associated with the anomaly high to the northeast of the plateau, are in favour of cyclonic winds shear to the east of the Tibetan Plateau. In short, in situation E, the negative geopotential height anomalies to the east of the Tibetan Plateau are stronger and more extensive, the anomalous high to the northeast of the plateau is located further south than that in situation W, and positive geopotential height anomalies are found over Southeastern China. The circulations in situation E aid in the maintenance of the moving-off TPVs, thereby contributing to the longer EPDs. Similar conditions are also observed at

700 hPa (Fig. 5), indicating coherent circulations in the middle and lower troposphere.

3.2. Upper troposphere

Considering that the wind speed anomalies at 200 hPa do not reflect the westerly jet stream clearly (figure not shown), the wind speed composites at 200 hPa based on the original data are provided in Fig. 6. Two jet stream cores are found to the north of the Tibetan Plateau and over Northeast Asia. Usually, divergence occurs at the entrance of the jet core at 200 hPa (Xuan et al., 2011; Jia and Yang, 2013). Thus, the jet core over Northeast Asia has a primary effect on the eastward propagation of TPVs. The jet core in situation E (Fig. 6b) is much stronger than that in situation W (Fig. 6a), resulting in a larger change in jet speed in the former. Accordingly, situation E (situation W) is more favourable (unfavourable) for divergence at 200 hPa. The configuration of the divergence fields in the upper and lower troposphere is closely related to vertical motion. Regarding lower-level conditions, as presented in Figs. 4 and 5, the extent of the negative geopotential height anomalies and the related convergence fields are greater in situation E.

Figure 7 shows the vertical motion associated with the upper-level divergence and lower-level convergence in both situations, which are averaged between 30°N and 40°N. The ascending motion stretches further eastward in situation E, which is in accordance with longer EPDs in situation E (Fig. 1). In addition, the vertical ascending motion is stronger and deeper in situation E, which is more favourable for the maintenance of TPVs and longer EPDs. The difference in vertical motion between the two situations is presented in Fig. 8, further verifying that the
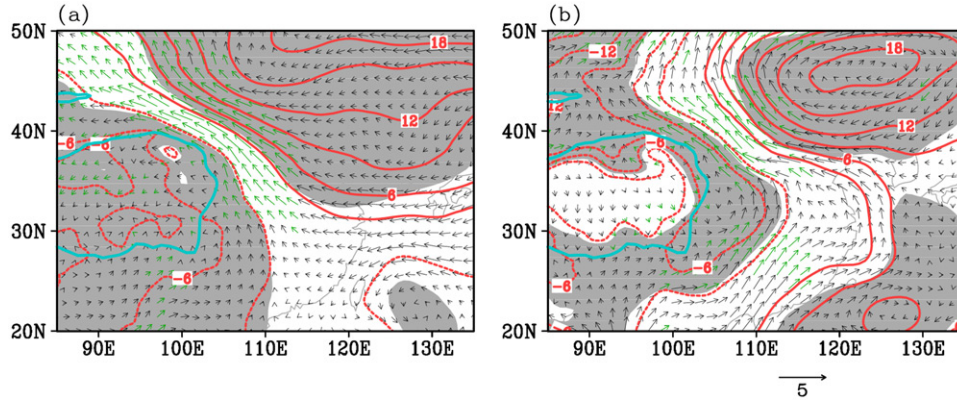
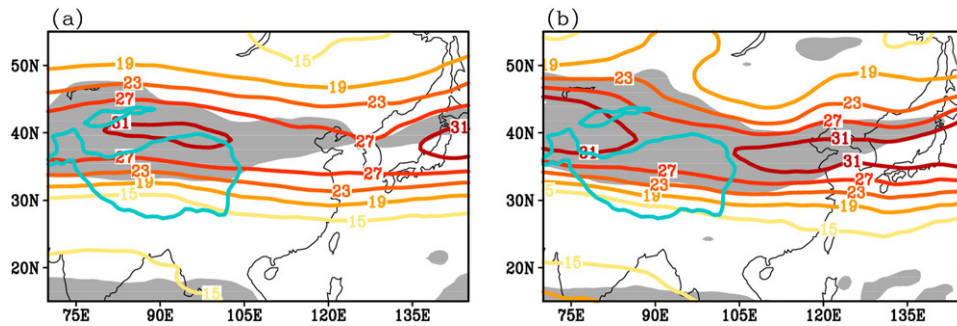*Fig. 5.* Same as Fig. 4 but for 700 hPa.

Fig. 6. Same as Fig. 4 but for wind speed (contours; unit: m s^{-1}) at 200 hPa. The wind speed exceeding the 90% confidence level is shaded.

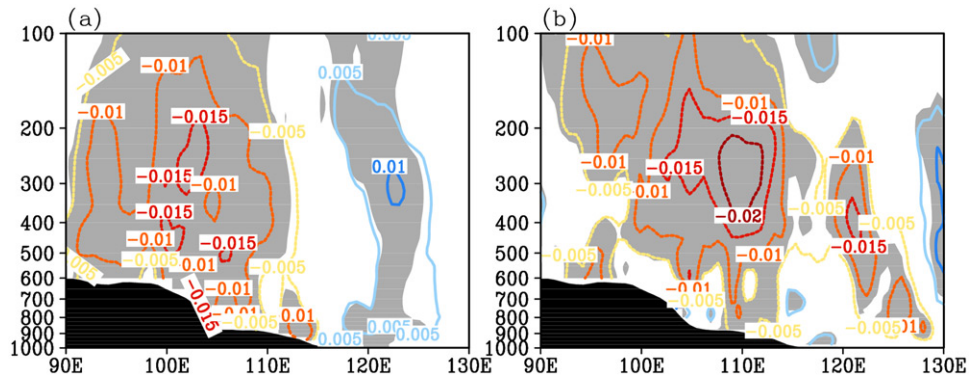*Fig. 7.* Height-longitudinal cross-sections of the anomalous vertical velocity (contours; unit: pa s^{-1}) averaged between 30°N and 40°N in (a) situation W and (b) situation E. The grey shadings represent the areas where the vertical velocity exceeds the 90% confidence level. Black shadings indicate the topography of the Tibetan Plateau.

ascending motion to the east of 110°E is significantly stronger in situation E than in situation W.

From the analyses above, the negative geopotential height anomalies in the middle and lower troposphere and the ascending motion to the east of the Tibetan Plateau associated with upper-level divergence and lower-level convergence are favourable for the maintenance of lows in this area, which benefits the eastward movement of TPVs. Thus, the

atmospheric dynamic features to the east of the Tibetan Plateau have a significant effect on the EPDs.

4. Atmospheric thermodynamic features

4.1. Atmospheric stratification conditions

To discuss the atmospheric stratification conditions to the east of the Tibetan Plateau, we calculate the potential
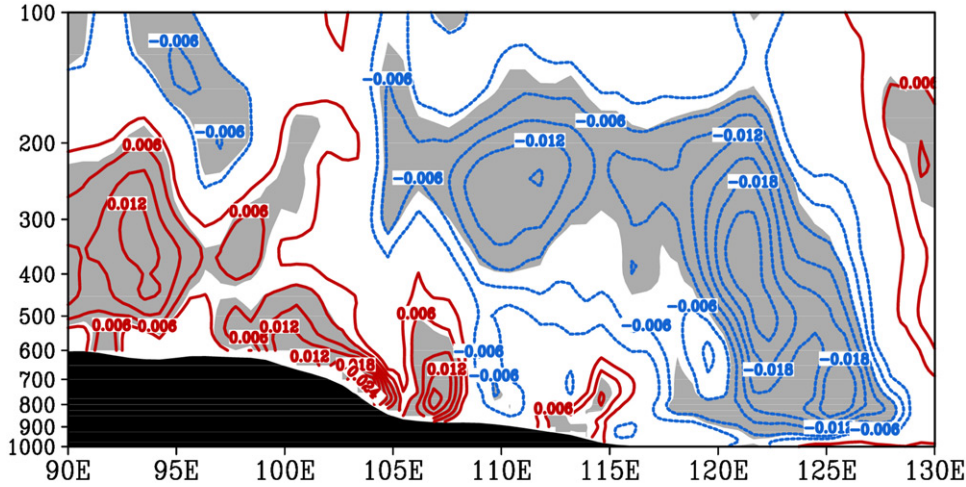
Fig. 8.   Height-longitudinal cross-sections of the difference in the anomalous vertical velocity averaged between 30°N and 40°N between situations E and W (contours; unit: pa s^{-1}). The grey shadings represent the areas where the difference exceeds the 90% confidence level. Black shadings indicate the topography of the Tibetan Plateau.
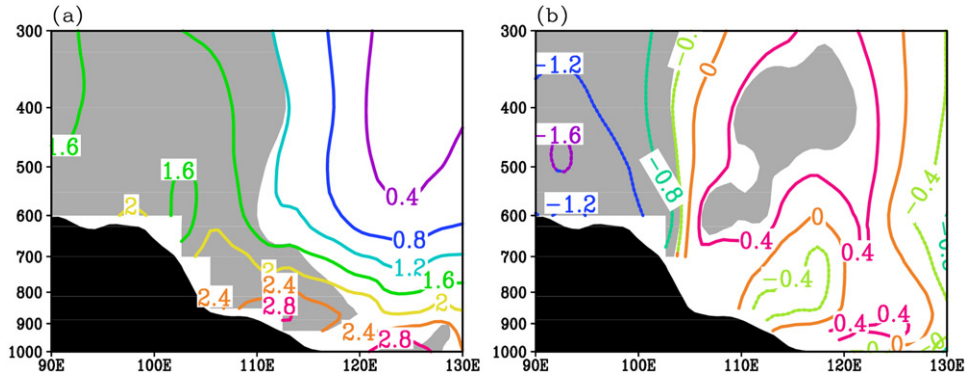

Fig. 9.   Same as Fig. 7 but for anomalous potential pseudo-equivalent temperature (θ_{se}) averaged between 30°N and 40°N (unit: K).

pseudo-equivalent temperature (θ_{se}). The height-longitude sections of the composites of θ_{se} anomalies averaged between 30°N–40°N for the two situations are given in Fig. 9. Because of the negligible specific humidity above 300 hPa and the weak θ_{se} above 300 hPa, the vertical distribution of the anomalous θ_{se} is given from 1000–300 hPa. Generally, the vertical gradient of θ_{se} reflects the instability of the atmosphere. To highlight the characteristics of atmospheric stratification, the climatological mean is removed. Accordingly, the vertical gradient of the θ_{se} anomalies indicates the relative instability of atmospheric stratification to the climatological mean. Thus, in this study, "unstable" and "stable" are actually relative conditions to the mean state. In Fig. 9, positive θ_{se} anomalies are found to the east of the Tibetan Plateau in both situations, with different ranges and locations of the centres. Generally, unstable atmospheric stratification aids in the development of TPVs, which are mainly sustained by the convective available potential energy in the

atmosphere (Wang, 1987). Unstable stratification is mainly located west of 110°E in situation W (Fig. 9a) and from 105°E to 120°E in situation E (Fig. 9b), indicating that the unstable conditions stretch further eastward in the latter situation. Therefore, the atmospheric stratification conditions to the east of 105°E in situation E contribute to longer EPDs.

However, a previous study (Wang, 1987) suggested that although unstable stratification is a favourable factor for the maintenance of TPVs, this stratification is unable to produce TPVs alone without water vapour. Since water vapour is also important for sustaining TPVs, we discuss the water vapour conditions related to both situations W and E in the next subsection.

4.2. Water vapour

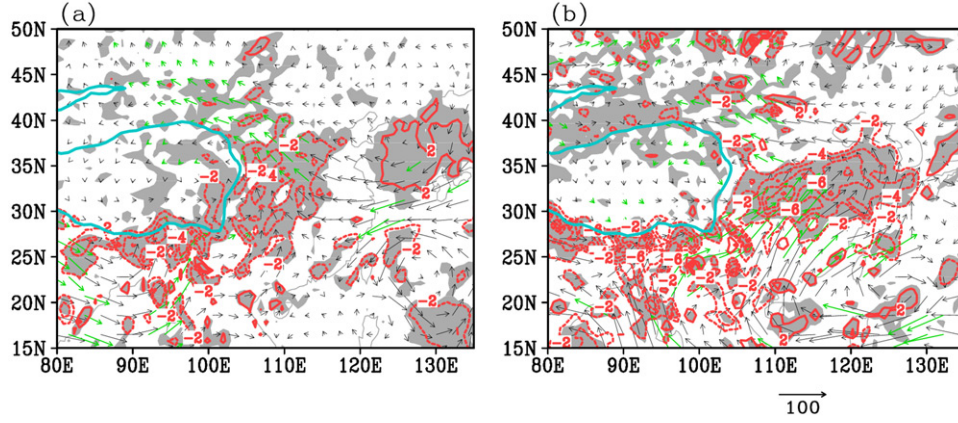Figure 10 shows the composites of the anomalous vertically integrated water vapour flux and water vapour flux

Fig. 10. Same as Fig. 4 but for the anomalous vertically integrated water vapour flux (vectors; unit: kg m^{-1} s^{-1}) and water vapour flux divergence (contours; unit: 10^{-5} kg m^{-2} s^{-1}). Water vapour flux and water vapour flux divergence anomalies with statistical significance exceeding the 90% confidence level are expressed by green vectors and shadings, respectively.
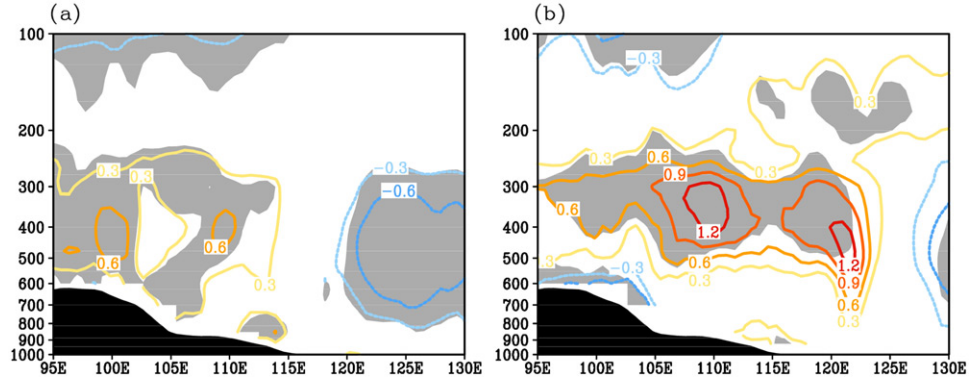

Fig. 11. Same as Fig. 7 but for the anomalous atmospheric apparent heat source (Q_1) averaged between 30°N and 40°N (unit: K d^{-1}).

divergence for situations W and E. Anomalous water vapour convergence is found to the east of the Tibetan Plateau in both situations, but the intensity is much greater in situation E. In situation W, the water vapour convergence area is observed from 100°E to 114°E, which is mainly induced by the water vapour transported from the West Pacific and the Bay of Bengal. In situation E, a broader region of water vapour convergence is observed over the middle and lower reaches of the Yangtze River, stretching further eastward compared with that in situation W. The stronger and more extensive water vapour convergence to the east of the Tibetan Plateau induced by water vapour from the South China Sea and Bay of Bengal in situation E corresponds to longer EPDs. Therefore, we infer that water vapour transport has a close relationship with the EPDs. Stronger and further eastward-stretching water vapour convergence leads to longer EPDs, and vice versa. The vectors of the water vapour flux in Fig. 10 coincide well with the winds anomalies at 500 and 700 hPa, as shown in Figs. 4 and 5,

respectively, indicating the importance of circulations in the middle and lower troposphere in water vapour transportation.

Considering that water vapour is a vital factor in triggering precipitation and that all of the dynamic and thermodynamic factors discussed in this study are closely related to precipitation and the latent heat of condensation, the heating features are discussed in the following subsection.

4.3. Atmospheric apparent heat source

The vertical structures and values of the atmospheric apparent heat source (Q_1) and the apparent moisture sink (Q_2) are similar (figure not shown), implying that the latent heat of condensational related to precipitation is a major component of Q_1. Here, the composites of the Q_1 anomalies averaged between 30°N–40°N for the two situations are shown in Fig. 11 to highlight the features of the heating structure. In both situations, positive Q_1
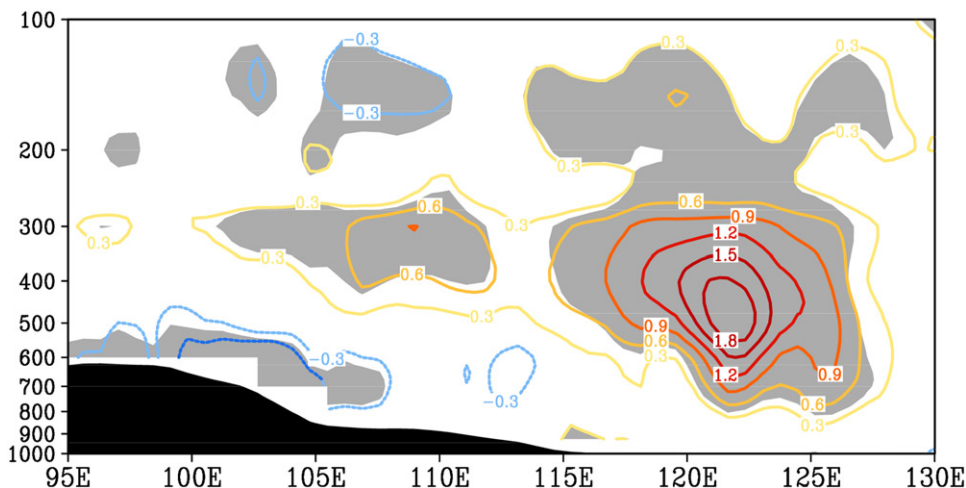
Fig. 12. Same as Fig. 8 but for the anomalous atmospheric apparent heat source (Q_I) averaged between 30°N and 40°N (unit: K d^{-1}).

anomalies occur over the eastern edge and to the east of the Tibetan Plateau, with the heating centres located above 500 hPa. Previous studies (Steenburgh and Holton, 1993; Hirschberg and Fritsch, 1993) have demonstrated that upper-level heating above 500 hPa lowers the 500 hPa isobaric surface, which is conducive to the maintenance of TPVs. The heating extent in the zonal direction above 500 hPa in situation W is located to the west of 115°E, whereas that in situation E stretches eastward to approximately 125°E, implying that heating affects a wider region in the zonal direction in the latter situation, which corresponds to longer EPDs. Furthermore, the difference in Q_I between the two situations presents stronger heating in situation E compared with situation W; this difference extends from the eastern Tibetan Plateau to 128°E, especially to the east of 115°E (Fig. 12). Thus, heating above 500 hPa may have an important causal effect on the eastward propagation of TPVs.

5. Summary and discussion

TPVs moving off the Tibetan Plateau have an important effect on precipitation over the regions to the east of the Tibetan Plateau. The previous work investigating the stage after the TPVs move off the Tibetan Plateau mainly focused on the influence of TPVs on precipitation and the large-scale circulations associated with TPVs. Actually, the precipitation areas associated with the moving-off TPVs are closely related to their eastward propagation distances. Accordingly, in the present study, pre-existing large-scale dynamic and thermodynamic features were investigated to provide a causal explanation for why some TPVs propagate further eastward than others. This is helpful for predicting the propagation distances of the

moving-off TPVs. Two groups of moving-off TPVs from May to August in 1998–2015 were selected by referring to the *Yearbook of Tibetan Plateau Vortex and Shear Line* from the Institute of Plateau Meteorology, CMA, according to their EPDs. The TPVs that dissipated west of 110°E were defined as group W, and those reaching beyond 110°E were defined as group E. The situations corresponding to these two groups of TPVs were labeled as "situation W" and "situation E", respectively. The large-scale circulations and thermodynamic conditions at the moving-off times in these two situations were compared. The main results are described as follows:

1. The atmospheric dynamic conditions to the east of the Tibetan Plateau significantly affect the EPDs.
    -   In the middle and lower troposphere, in situation E, the stronger anomalous low to the east of the Tibetan Plateau, the anomalous high to the northeast of the plateau which is located further south, and the stronger WPSH, promote the maintenance of the moving-off TPVs, contributing to longer EPDs in situation E than in situation W.
    -   At 200 hPa, the jet stream cores located over Northeast Asia act as a primary influence on the eastward movement of the TPVs in both situations, an effect that is stronger in situation E. The upper-level divergence associated with the jet stream cores is favourable for the ascending motion to the east of the Tibetan Plateau under the coaction of convergence in the middle and lower troposphere. Accordingly, the higher intensity and wider range of ascending motion in the zonal direction is observed in situation E, corresponding to longer EPDs.

2. The thermodynamic factors exhibit an important influence on the EPDs.
   - In situation E, unstable stratification stretches further eastward, and anomalous water vapour convergence exhibits a larger extent in the zonal direction, which is in accordance with the longer EPDs.
   - Heating fields are observed to the east of the Tibetan Plateau in both situations W and E, with centres located above 500 hPa. The upper-level heating lowers the 500 hPa isobaric surface, benefiting the maintenance and eastward movement of TPVs. In situation E, the upper-level heating stretches further eastward, corresponding to longer EPDs; the smaller heating range in the zonal direction in situation W is consistent with shorter EPDs.

Overall, the EPDs are considerably longer when the ranges of the favourable dynamic and thermodynamic conditions mentioned above stretch further eastward in the zonal direction, and vice versa.

It should be noted that the TPVs detected in the yearbooks are manually obtained from observational sounding stations, whose observation intervals are 12 h. Due to the low temporal and spatial station coverage across the Tibetan Plateau, it is difficult to track TPVs and be sure that a TPV observed at one time step is the same TPV as observed 12 h ago. Therefore, further examination based on higher resolution data is needed. In addition, the manual tracking of TPVs in this work is subjective, thus, the objective tracking method (Curio et al., 2018; Curio et al., 2019) should be utilized in future work, which is beneficial for the climatological study of TPVs. Moreover, although the dynamic and thermodynamic effects on EPDs are revealed in this work, questions remain regarding their relative roles and the different mechanisms involved before, during, and after moving off the Tibetan Plateau. These questions require further research in the forms of calculating the diagnostic equations and performing numerical experiments.

Disclosure statement

No potential conflict of interest was reported by the authors.

Funding

References

Chen, B. M., Qian, Z. A. and Zhang, L. S. 1996. Numerical simulation of formation and development of vortices over the Qinghai-Xizang Plateau in summer. *Chin. J. Atmos. Sci.* **20**, 491–502 (in Chinese)

Curio, J., Chen, Y. R., Schiemann, R., Turner, A. G., Wong, K. C. and co-authors. 2018. Comparison of a manual and an automated tracking method for Tibetan Plateau vortices. *Adv. Atmos. Sci.* **35**, 965–980. doi:10.1007/s00376-018-7278-4

Curio, J., Schiemann, R., Hodges, K. I. and Turner, A. G. 2019. Climatology of Tibetan Plateau vortices in reanalysis data and a high-resolution global climate model. *J. Climate* **32**, 1933–1950. doi:10.1175/JCLI-D-18-0021.1

Dee, D. P., Uppala, S. M., Simmons, A. J. Berrisford, P., Poli, P. and co-authors. 2011. The ERA-Interim reanalysis: Configuration and performance of the data assimilation system. *Q. J. R. Meteor. Soc.* **137**, 553–597.

Dell'Osso, L. and Chen, S. J. 1986. Numerical experiments on the genesis of vortices over the Qinghai-Xizang Plateau. *Tellus* **38A**, 235–250.

Gao, W. L. and Yu, S. H. 2007. Analyses on mean circulation field of the plateau low vortex moving out of the Tibetan Plateau. *Plateau Meteor.* **26**, 206–212 (in Chinese)

Gu, Q. Y., Shi, R. and Xu, H. M. 2010. Comparison analysis of the circulation characteristics of plateau vortex moving out of and not out of the plateau. *Meteor. Mon.* **36**, 7–15 (in Chinese)

Guo, M. Z. 1986. General investigation of the moving eastward Lows over Qinghai-Xizang Plateau. *Plateau Meteor.* **5**, 184–188 (in Chinese).

Hirschberg, P. A. and Fritsch, J. M. 1993. On understanding height tendency. *Mon. Wea. Rev.* **121**, 2646–2661. doi:10.1175/1520-0493(1993)121<2646:OUHT>2.0.CO;2

Huang, C. H., Li, G. P., Niu, J. L., Zhao, F. H., Zhang, H. and co-authors. 2015. A 30-year climatology of the moving-out Tibetan plateau vortex in summer and its influence on the rainfall in china. *J. Tropical Meteor.* **31**, 827–838.

Jia, X. L. and Yang, S. 2013. Impact of the quasi-biweekly oscillation over the western North Pacific on East Asian subtropical monsoon during early summer. *J. Geophys. Res. Atmos.* **118**, 4421–4434. doi:10.1002/jgrd.50422

Lhasa Group for Tibetan Plateau Meteorology Research. 1981. *Research of 500 hPa Vortices and Shear Lines over the Tibetan Plateau in Summer*. Science Press, Beijing, p. 122 (in Chinese).

Li, G. P. 2002. *The Tibetan Plateau Dynamic Meteorology*. China Meteorological Press, Beijing, p. 271 (in Chinese).

Li, G. P. and Zhao, B. J. 2002. A dynamical study of the role of surface sensible heating in the structure and intensification of the Tibetan Plateau vortices. *Chin. J. Atmos. Sci.* **26**, 519–525 (in Chinese)

Li, G. P., Zhao, H. H., Huang, C. H. and Niu, J. L. 2014. Analysis of 30-year climatology of the Tibetan Plateau vortex

in summer with NCEP reanalysis data. *Chin. J. Atmos. Sci.* **38**, 756–769 (in Chinese).

Li, L., Zhang, R. H. and Wen, M. 2011. Diagnostic analysis of the evolution mechanism for a vortex over the Tibetan Plateau in June 2008. *Adv. Atmos. Sci.* **28**, 797–808. doi:10.1007/s00376-010-0027-y

Li, L., Zhang, R. H. and Wen, M. 2014. Diurnal variation in the occurrence frequency of the Tibetan Plateau vortices. *Meteorol. Atmos. Phys.* **125**, 135–144. doi:10.1007/s00703-014-0325-5

Li, L., Zhang, R. H., Wen, M. and Liu, L. K. 2014. Effect of the atmospheric heat source on the development and eastward movement of the Tibetan Plateau vortices. *Tellus A* **66**, 24451. doi:10.3402/tellusa.v66.24451

Li, L., Zhang, R. H. and Wen, M. 2017. Genesis of southwest vortices and its relation to Tibetan Plateau vortices. *Q. J. R. Meteorol. Soc.* **143**, 2556–2566. doi:10.1002/qj.3106

Li, L., Zhang, R., Wen, M. and Lü, J. 2018. Effect of the atmospheric quasi-biweekly oscillation on the vortices moving off the Tibetan Plateau. *Clim. Dyn.* **50**, 1193–1207. doi:10.1007/s00382-017-3672-3

Li, L., Zhang, R. H., Wen, M. and Duan, J. P. 2019. Development and eastward movement mechanisms of the Tibetan Plateau vortices moving off the Tibetan Plateau. *Clim. Dyn.* **52**, 4849–4859. doi:10.1007/s00382-018-4420-z

Liu, F. M. and Fu, M. J. 1985. A study on the moving eastward Lows over Qinghai-Xizang Plateau. *Plateau Meteor.* **5**, 125–134 (in Chinese).

Luo, S. W., Yang, Y. and Lu, S. H. 1991. Diagnostic analyses of a summer vortex over Qinghai-Xizang Plateau for 29–30 June 1979. *Plateau Meteor.* **10**, 1–11.

Luo, S. W. 1992. *Study on Some Kinds of Weather Systems over and around the Qinghai-Xizang Plateau.* China Meteorological Press, Beijing, p. 205 (in Chinese).

Luo, S. W. and Yang, Y. 1992. A case study on numerical simulation of summer vortex over Qinghai-Xizang (Tibetan) Plateau. *Plateau Meteor.* **11**, 39–48.

Luo, S. W., He, M. L. and Liu, X. D. 1994. Study on the vortex of the Qinghai-Xizang (Tibet) Plateau in summer. *Sci. China Ser. B* **37**, 601–612. doi:

Qiao, Q. M. and Zhang, Y. G. 1994. *Synoptic Meteorology of the Tibetan Plateau and Its Effect on the near Areas.* China Meteorological Press, Beijing, p. 251 (in Chinese).

Rasmusson, E. M. 1968. Atmospheric water vapor transport and the water balance of north America II. Large scale water balance investigations. *Mon. Wea. Rev.* **96**, 720–734. doi:10.1175/1520-0493(1968)096<0720:AWVTAT>2.0.CO;2

Shen, R. J., Reiter, E. R. and Bresch, J. F. 1986. Some aspects of the effects of sensible heating on the development of summer weather system over the Qinghai-Xizang Plateau. *J. Atmos. Sci.* **43**, 2241–2260. doi:10.1175/1520-0469(1986)043<2241:SAOTEO>2.0.CO;2

Steenburgh, W. J. and Holton, J. R. 1993. On the interpretation of geopotential height tendency equations. *Mon. Wea. Rev.* **121**, 2642–2645. doi:10.1175/1520-0493(1993)121<2642:OTIOGH>2.0.CO;2

Tang, X. Y., Zhou, C. Y. and Wang, G. 2014. Statistical analysis on the plateau low vortex activity characteristics. *Plateau Mount. Meteorol. Res.* **34**, 41–44 (in Chinese).

Wang, B. 1987. The development mechanism for Tibetan Plateau warm vortices. *J. Atmos. Sci.* **44**, 2978–2994. doi:10.1175/1520-0469(1987)044<2978:TDMFTP>2.0.CO;2

Wang, X., Li, Y. Q., Yu, S. H. and Jiang, X. W. 2009. Statistical study on the plateau low vortex activities. *Plateau Meteor.* **28**, 64–71 (in Chinese).

Xiao, D. X., Yu, S. H. and Tu, N. N. 2016. Analysis of typical sustained plateau vortexes after departure. *Plateau Meteor.* **35**, 43–54 (in Chinese).

Xuan, S. L., Zhang, Q. Y. and Sun, S. Q. 2011. Anomalous midsummer rainfall in Yangtze River-Huaihe River Valleys and its association with the East Asia westerly jet. *Adv. Atmos. Sci.* **28**, 387–397. doi:10.1007/s00376-010-0111-3

Yanai, M., Steven, E. and Chu, J. H. 1973. Determination of bulk properties of tropical cloud clusters from large scale heat and moisture budgets. *J. Atmos. Sci.* **30**, 611–627. doi:10.1175/1520-0469(1973)030<0611:DOBPOT>2.0.CO;2

Ye, D. Z. and Gao, Y. X. 1979. *The Tibetan Plateau Meteorology.* Science Press, Beijing, p. 278 (in Chinese).

Yu, S. H. 2002. Water vapor imagery of vortex moving process over Qinghai-Xizang Plateau. *Plateau Meteor.* **21**, 199–204 (in Chinese).

Yu, S. H. and Gao, W. L. 2006. Observational analysis on the movement of vortices before/after moving out the Tibetan Plateau. *Acta Meteor. Sin.* **64**, 392–399. doi:10.11676/qxxb2006.038 (in Chinese).

Yu, S. H., Gao, W. L. and Gu, Q. Y. 2007. The middle-upper circulation analyses of the Plateau low vortex moving out of Plateau and influencing flood in east China in recent years. *Plateau Meteor.* **26**, 466–475 (in Chinese).

Yu, S. H., Gao, W. L. and Peng, J. 2012. Statistical analysis on influence of Qinghai-Xizang Plateau vortex activities on precipitation in China. *Plateau Meteor.* **31**, 592–604 (in Chinese).

Yu, S. H., Gao, W. L., Peng, J. and Xiao, Y. H. 2014. Observational facts of sustained departure plateau vortexes. *J. Meteorol. Res.* **28**, 296–307. doi:10.1007/s13351-014-3023-9

Yu, S. H., Gao, W. L. and Peng, J. 2015. Circulation features of sustained departure plateau vortex at middle tropospheric level. *Plateau Meteor.* **34**, 1540–1555 (in Chinese)